Numerical Simulation of a Single-Mode Sinusoidal Flame Interacting with a Shockwave

Wei Wei, Bing Wang*
School of Aerospace Engineering, Tsinghua University
Beijing, China

1 Extended Abstracts

In the 1960s, Richtmyer analyzed the Taylor instability in a shock acceleration of compressible fluids firstly using the theoretical method [1]. Then Meshkov validated Richtmyer's prediction in the shocktube experiments [2]. Since then, various research on the instability of multi-fluids with different densities induced by the impaction of shock waves, called Richtmyer-Meshkov instability (RMI), has been conducted to predict the development of the fluid interface and reveal the physical mechanism of the disturbance growth.

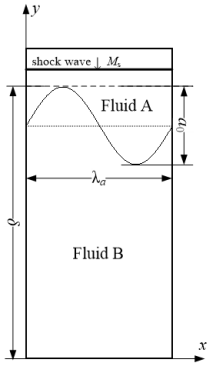

Figure 1. Sketch of the physical model.

Literature investigation shows that, lots of experiments and numerical simulations [3-6] have been done on the RMI of inert fluid. Few study has been conducted in chemically reactive fluids in the past decades, especially in regards to the evolution of the shocked interface considering its detailed chemistry. In this paper, a numerical study is performed on the Richtmyer-Meshkov instability of a single-mode sinusoidal interface in chemically reactive fluids. The computation model is shown in figure 1. The perturbed flame is initially generated by a premixed combustion of the H_2/O_2 reactive mixture, and then the RMI would be

Correspondence to: wbing@tsinghua.edu.cn

triggered by the incident shock wave introduced from combustion product fluids. After the interaction between the shockwave and flame surface, the amplitude of the interface would grow and the reaction rate would increase.

The multi-species reactive Navier-Stokes equations are solved,

$$\frac{\partial \rho}{\partial t} + \frac{\partial \rho u_j}{\partial x_j} = 0 \tag{1}$$

$$\frac{\partial \rho u_i}{\partial t} + \frac{\partial (\rho u_i u_j + p\delta_{ij})}{\partial x_j} = \frac{\partial \tau_{ij}}{\partial x_j} \tag{2}$$

$$\frac{\partial \rho E}{\partial t} + \frac{\partial (\rho E u_j + p u_j)}{\partial x_j} = \frac{\partial \left(u_j \tau_{ij} + q_j\right)}{\partial x_j} \tag{3}$$

$$\frac{\partial \rho Y_k}{\partial t} + \frac{\partial \rho Y_k u_j}{\partial x_j} = \frac{\partial}{\partial x_j}(\rho D_k \frac{\partial Y_k}{\partial x_j}) + \dot{\omega}_k \tag{4}$$

where ρ, u_i, p, E, and Y_k are the density, the velocity in the i^{th} direction, the pressure, the total energy and the mass fraction of the k^{th} species respectively.

$$\tau_{ij} = \mu(\frac{\partial u_i}{\partial x_j} + \frac{\partial u_j}{\partial x_i} - \frac{2}{3}\frac{\partial u_k}{\partial x_k}\delta_{ij})$$

is the viscous stress;

$$q_j = -\lambda \frac{\partial T}{\partial x_j} + \sum_k \rho h_k D_k \frac{\partial Y_k}{\partial x_j}$$

is the heat flux. μ, λ and D_k denote the molecular viscosity, thermal conductivity and the diffusion coefficient of species k respectively, which are computed using the empirical formulas [7]. $\dot{\omega}_k$ is the reaction rate of production of species k, and a detailed chemical reaction mechanism containing of 9 species and 19 steps is adopted [8].

The fifth-order WENO scheme [9] is used to compute the convection terms, and a point implicit method is used for the source term. The viscous diffusion terms are computed by a sixth-order symmetric compact scheme. The time integration of the discretized equations is performed by an explicit third-order Runge-Kutta method.

An inert RMI case was firstly simulated under different grid resolutions to validate the present numerical procedures, using the flow parameters in the experiment conducted by Jacobs and Krivets [10]. The initial conditions of the experimental setup considered in the present numerical study are as follows: The shock wave has a strength of M_s =1.3 in air. The sinusoidal interface of air-SF_6 has a pre-shock amplitude of a_0 = 2.9 mm and a wavelength of λ_a = 59 mm. The Atwood number is At = 0.605.

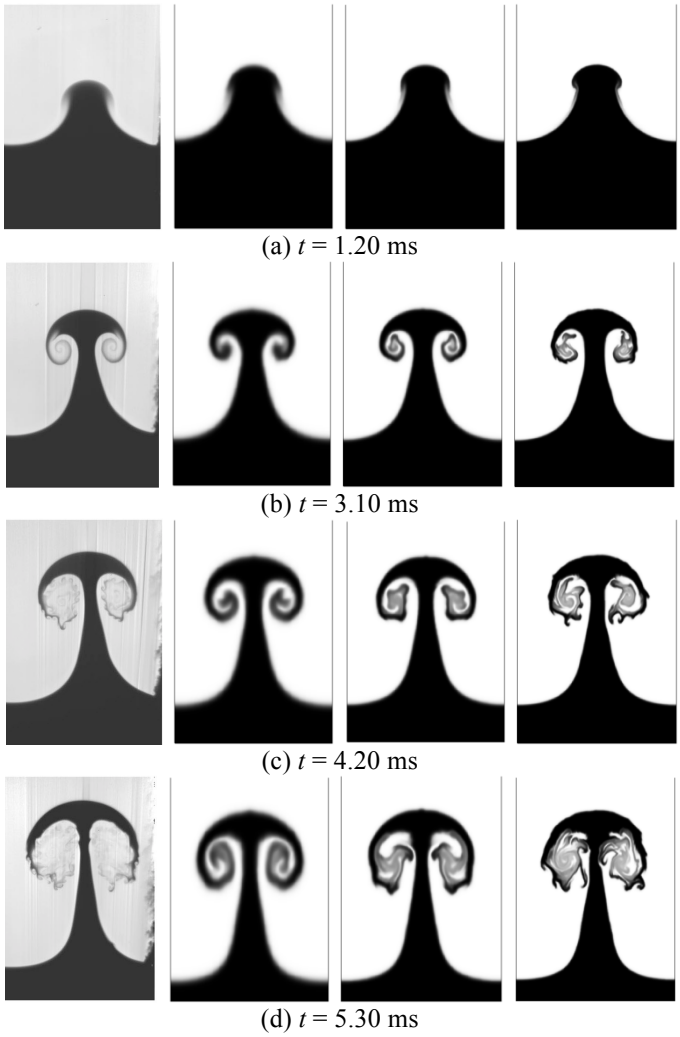

(a) t = 1.20 ms

(b) t = 3.10 ms

(c) t = 4.20 ms

(d) t = 5.30 ms

Figure 2. Comparison of the experimental results of Jacobs and Krivets [10] (left) and the present numerical results under three different grid sizes: Δx = 0.5 mm (middle left), Δx = 0.25 mm (middle right), Δx = 0.125 mm (right).

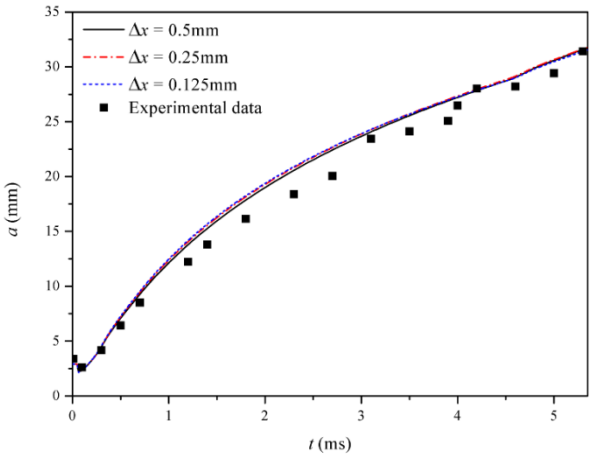

Figure 3. The amplitude of the interface changing with the time.

The SF_6 mass fraction distribution is compared to the experimental results, as shown in figure 2. As the increase of the resolution, there are more and more small structures, while the main stuctures remains almostly the same. This can also be seen from the profiles of amplitude of the interface, as shown in figure 3. The three profiles of the amplitude are almost coincident, and they are slightly different from the experimental data, which is due to the error of thermodynamic model.

After the validation, the reactive cases are studied with different parameters qualitatively and quantitatively to reveal the growth mechanism of disturbance. The detailed results will be presented in the final paper.

It was found that the competition of baroclinic effects with the reaction heat release determines the interface evolution. The reaction induction time of shocked unburned fluids decreases and the apparent flame propagation advances if the strength of the incident shock wave increases, thereby leading to a faster chemical reaction. The interface growth will enter the non-linear status earlier as the initial amplitude of the single-mode interface increases. The rollups of mushrooms, representative of unstable flow structures, are accelerated and spatially spread the reaction in the fresh fluids through a stronger incident shock wave. The fast chemical reaction due to the high mixture temperature will consume the unburned fluids in the small-scale structures, where a higher concentration of radical OH is distributed, and the flame will thicken. The enstrophy is mainly generated on the interface and exhibits increased oscillation, which demonstrates that the impaction of the baroclinic effects of shock wave is greater than that of the dilatation on the increased vorticity.

References

[1] Richtmyer R D. (1954). Taylor instability in shock acceleration of compressible fluids. Communications on Pure & Applied Mathematics. 13(2):297-319.

[2] Meshkov E E. (1969). Instability of the interface of two gases accelerated by a shock wave. Fluid Dynamics. 4(5):101-104.

[3] Collins B D, Jacobs J W. (2002). PLIF flow visualization and measurements of the Richtmyer-Meshkov instability of an air/SF6 interface. Journal of Fluid Mechanics. 464:113-136.

[4] Prestridge K, Orlicz G, Balasubramanian S, et al. (2013). Experiments of the Richtmyer-Meshkov instability. Philosophical Transactions. Series A, Mathematical, Physical, and Engineering Science. 371:1-9.

[5] Holmes R L. (1994). A numerical investigation of the Richtmyer-Meshkov instability using Front Tracking. Journal of Fluid Mechanics. 301: 51-64.

[6] Latini M, Schilling O, Don W S. (2006). Effects of WENO flux reconstruction order and spatial resolution on reshocked two-dimensional Richtmyer-Meshkov instability. Journal of Computational Physics. 221:805-836.

[7] Poling B E, Prausnitz J M, O'Connell J P. (2000) The Properties of gases and liquids. Physics Today. 24(24):38.

[8] Tien J H, Stalker R J. (2002). Release of chemical energy by combustion in a supersonic mixing layer of hydrogen and air. Combustion and Flame. 131(3): 329-348.

[9] Shu C W, Osher S. (1989). Efficient implementation of essentially non-oscillatory shock-capturing schemes. Journal of Computional Physics. 83:32–78.

[10] Jacobs J W, Krivets V V. (2005). Experiments on the late-time development of single-mode Richtmyer–Meshkov instability. Physics of Fluids. 17(3):93-106.